ELSEVIER

Biophysical Chemistry 107 (2004) 243–253

Biophysical Chemistry

www.elsevier.com/locate/bpc

Requirements for generating sigmoidal time–course aggregation in nucleation-dependent polymerization model

Masato Kodaka*

Institute for Biological Resources and Functions, National Institute of Advanced Industrial Science and Technology (AIST), Tsukuba Central 6, 1-1-1 Higashi, Tsukuba, Ibaraki 305-8566, Japan

Received 13 May 2003; received in revised form 25 August 2003; accepted 4 September 2003

Abstract

Requirements for generating remarkable sigmoidal time–course of aggregation are found in the nucleation-dependent polymerization model by a numerical calculation method; i.e. there are optimum values of the kinetic constants to afford prominent sigmoidal character by inducing slightly unfavorable nucleation. However, if the nucleus formation is too unfavorable, sigmoidal character is again decreased. This result is in contrast to the generally accepted idea that sigmoid is induced by thermodynamically unfavorable nucleation phase.

Keywords: Nucleation-dependent polymerization model; Sigmoid; Kinetic constants

1. Introduction

Spontaneous formation of fibrils with specific β-sheet structures (amyloid fibrils) from soluble proteins is very important to understand fundamental mechanisms of protein folding and conformational diseases such as the Alzheimer's disease [1,2] and prion disease [3,4]. One of the typical kinetic characteristics in amyloid fibril formation is a sigmoidal time–course curve with an initial lag time (or an induction period). Studies on sigmoidal nature are important, because this nature reflects the degree of cooperation in the process of fibril formation. Namely, the sigmoidal nature is more prominent as the degree of cooperation is larger. Therefore, the analysis of the sigmoidal nature is expected to contribute to the understanding of the mechanism of amyloid fibril formation. The so-called nucleation-dependent polymerization model has been generally used to analyze its mechanism, which is composed of an initial nucleation phase and an elongation (extension) phase as shown in Scheme 1 [5]. It has been extensively believed that the sigmoidal behavior is caused by thermodynamically unfavorable nuclear formation and fast elongation [5,6]. In spite of extensive citation of this well-known explanation, there have been no definite evidences showing the validity of this interpretation. In the nucleation-dependent polymerization model, lots of differential equations must be solved simultaneously to obtain time–course curves of individual aggregation species. The most straightforward and correct way to solve the differential equations is numerical calculations,

*Tel.: +81-29-861-6124; fax: +81-29-861-6123.
E-mail address: m.kodaka@aist.go.jp (M. Kodaka).

0301-4622/04/$ - see front matter © 2003 Elsevier B.V. All rights reserved.
doi:10.1016/j.bpc.2003.09.013

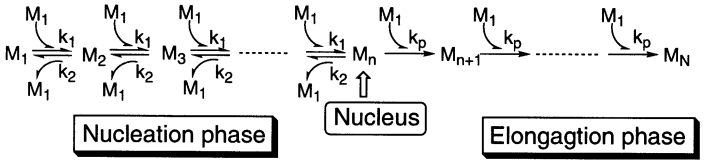

Nucleation-Dependent Polymerization Model

Scheme 1.

because it is impossible to solve them in analytical methods without approximation.

In the present study, the true meaning of nucleation-dependent polymerization mechanism is pursued. A notable finding is that there are optimal values of the rate constants to give remarkable sigmoidal character, which is different from the conventionally accepted simple interpretation. Though experimental evidences are not available, the present conclusion is expected to contribute to the interpretation of the cooperative behavior not only in amyloid fibril formation but also in various aggregation systems.

2. Calculation

In the nucleation-dependent polymerization model shown in Scheme 1, the following differential equations Eqs. (1)–(5) hold, assuming that the nucleus is 10-mer, the aggregate larger than 10-mer is regarded as fibril, and the elongation proceeds up to *N*-mer. It has been confirmed that the fundamental conclusion of the present study is not influenced by the size of the nucleus. Eqs. (1)–(5) were derived by considering the increasing rate of the concentration for the individual species $[M_j]$ $(j=1–N)$,

$$\frac{d[M_1]}{dt} = -k_1[M_1]\left(2[M_1]+\sum_{j=2}^{9}[M_j]\right) + k_2\left(2[M_2]+\sum_{j=3}^{10}[M_j]\right) - k_p[M_1][M_{10}] - k_p[M_1][P] \quad (1)$$

$$\frac{d[M_j]}{dt} = k_1[M_1]\left([M_{j-1}]-[M_j]\right) - k_2\left([M_j]-[M_{j+1}]\right) \quad (j=2-9) \quad (2)$$

$$\frac{d[M_{10}]}{dt} = k_1[M_1][M_9]-k_2[M_{10}]-k_p[M_1][M_{10}] \quad (3)$$

$$\frac{d[M_j]}{dt} = k_p[M_1]\left([M_{j-1}]-[M_j]\right) \quad (j=11 \text{ to } N-1) \quad (4)$$

$$\frac{d[M_N]}{dt} = k_p[M_1][M_{N-1}] \quad (5)$$

where $[P]$ signifies the concentration of fibrils from $j=11$ to $N-1$, viz., $[P]=\sum_{j=11}^{N-1}[M_j]$.

The total concentration of the monomers incorporated into fibrils is given by Eq. (6).

$$[F]=\sum_{j=11}^{N} j[M_j]. \quad (6)$$

In the special case that *N* is infinity, the following differential equations Eqs. (7)–(11) are obtained in view of the increasing rate of the concentration for the individual species $[M_j]$ $(j=1–10)$, the concentration of fibrils $[P]$ and the total concentration of the monomers incorporated into fibrils $[F]$. It is obvious that the increasing rate of $[P]$ is given by Eq. (10), since it is equal to the increasing rate of $[M_{11}]$. Furthermore, the increasing rate of $[F]$

is shown by Eq. (11), where the first term indicates the binding rate of monomer to the fibrils and the second term means the binding rate of monomer to M_{10} to form M_{11}.

$$\frac{d[M_1]}{dt} = -k_1[M_1]\left(2[M_1] + \sum_{j=2}^{9}[M_j]\right) + k_2\left(2[M_2] + \sum_{j=3}^{10}[M_j]\right) - k_p[M_1][M_{10}] - k_p[M_1][P] \quad (7)$$

$$\frac{d[M_j]}{dt} = k_1[M_1]\left([M_{j-1}] - [M_j]\right) - k_2\left([M_j] - [M_{j+1}]\right) \quad (j = 2-9) \quad (8)$$

$$\frac{d[M_{10}]}{dt} = k_1[M_1][M_9] - k_2[M_{10}] - k_p[M_1][M_{10}] \quad (9)$$

$$\frac{d[P]}{dt} = k_p[M_1][M_{10}] \quad (10)$$

$$\frac{d[F]}{dt} = k_p[M_1][P] + 11k_p[M_1][M_{10}] \quad (11)$$

where $[P]$ denotes the concentration of fibrils, viz., $[P] = \sum_{j=11}^{\infty}[M_j]$.

In these calculations, the initial concentrations are $[M_1]_0 = 100$ (an arbitrary unit), $[M_j]_0 = 0$ ($j = 2$–N), $[P]_0 = 0$ and $[F]_0 = 0$. The differential Eqs. (1)–(5), (7)–(11) can be numerically solved by using MATHEMATICA (version 3.0, Wolfram Research, Inc.) for various k_2, k_p and N values under $k_1 = 1$ (an arbitrary unit). Fraction of fibril formation [f(%)] is thus obtained by Eq. (12).

$$f = 100[F]/[M_1]_0 = [F]. \quad (12)$$

3. Results

3.1. Relation between k_2 and n

Fig. 1a–c, respectively, show examples of time-course fibril formation in infinite elongating phase ($N = \infty$) for various k_2 (1, 100 and 500) under $k_p = 10\,000$, where the curves are found to be well represented by a stretched exponential function (Eq. (13)).

$$f = A\{1 - \exp(-Bt^n)\} \quad (13)$$

Here Fig. 1b gives higher sigmoidal character than Fig. 1a and c. Since the parameter n of Eq. (13) is an appropriate index measuring the degree of sigmoidal character, the dependence of n on k_2 was investigated in detail as shown in Fig. 2. When k_p is 10 000 and N is ∞ (Fig. 2a), the n value is almost constant (≈ 1.4) in $0.01 < k_2 < 1$, which means that the degree of sigmoidal property is not large in this region. The n value increases from 1.4 to 3.2 in $1 < k_2 < 100$ and then decrease from 3.2 to 1.3 in $100 < k_2 < 1000$. The noteworthy result is that there is the maximal n value (3.2) at $k_2 \approx 100$. Obviously, this result does not agree with the generally believed idea that thermodynamically unfavorable nuclear formation (viz. very large k_2) is a reason for generating sigmoidal curves [5,6]. As the N value is decreased from ∞ to 200, the maximum n value is also decreased and the corresponding k_2 value is shifted to smaller side. A similar tendency is observed when k_p is 1000 or 100 (Fig. 2b and c), while the maximal regions almost disappear at $k_p = 1$ (Fig. 2e). The above-mentioned phenomenon that the dependence of n on k_2 has a maximum can also be observed when the nucleus size is changed to 5 and 30, where the n value at the maximum position is increased as the nucleus size is increased; i.e. $n = 2.6$ at $k_2 = 500$ (nucleus size = 5), $n = 3.2$ at $k_2 = 100$ (nucleus size = 10), $n = 5.4$ at $k_2 = 5$ (nucleus size = 30).

3.2. Relation between k_p and n

Fig. 3a shows the relation between k_p and n at $k_2 = 100$. For infinite N, the n value monotonously increases with k_p. For $N = 200$ or 100, on the contrary, the n value tends to decrease with k_p. At $k_2 = 10$ (Fig. 3b), one can see the maximal regions at approximately $k_p = 30$ when N is ∞, 200 or 100. A similar tendency is observed at $k_2 = 1$ (Fig. 3c), while the maximal values are lower. For $N = 20$, the n value is essentially independent of k_p in $1 \leqq k_2 \leqq 100$.

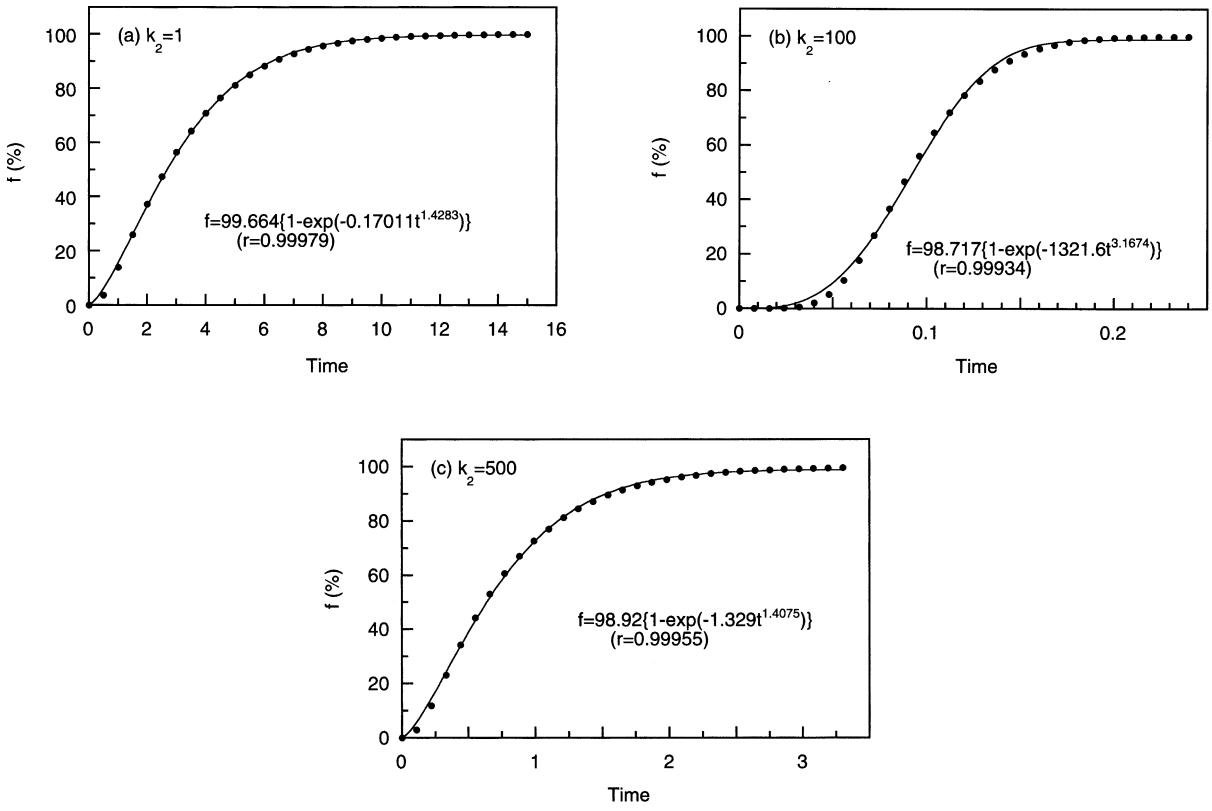

Fig. 1. Time-course of fibril formation for $k_p = 10\,000$ and $N = \infty$: (a) $k_2 = 1$; (b) 100 and (c) 500. The data are fitted by stretched exponential functions shown in the figures.

3.3. Relation between k_2 and $t_{1/2}$

Eq. (14) is derived from Eq. (13).

$$t_{1/2} = (\ln 2/B)^{1/n} \tag{14}$$

where $t_{1/2}$ signifies the time achieving 50% yield of fibril formation. Fig. 4 shows the relation between k_2 and $t_{1/2}$ for $1 \leqq k_p \leqq 10\,000$. A specially noticeable point is that minimal points exist in the region of $10 \leqq k_2 \leqq 100$, which well corresponds to the position where the maximal n is observed (Fig. 2). Namely, the larger the parameter n is, the faster the fibril formation proceeds. There is also a tendency that the $t_{1/2}$ values at the maximum points are decreased (namely, the aggregation becomes faster) as N is increased from 20 to ∞ and as k_p is increased from 1 to 10 000.

3.4. Time-course concentration of individual species

To reveal the reason for generating sigmoidal curves, the kinetic mechanism was analyzed in more detail by observing the time–course concentration of the individual species ($[M_j]$) and the fibrils ($[P]$). Fig. 5a–d exhibit the changes in the concentrations of monomer (M_1), dimer (M_2), nucleus (M_{10}) and fibril (P) for various k_2 values (0.01, 1, 100 and 1000) under $k_p = 1000$ and $N = \infty$. When k_2 is small (0.01) (Fig. 5a), the concentration of the monomer M_1 drops steeply to a very low level ($< 2 \times 10^{-2}$), followed by the rapid formation of M_2. The nucleus (M_{10}) is formed slowly and has the maximum when the time is approximately 200. Concomitant with this, the concentration of the elongating fibrils $[P]$ increases

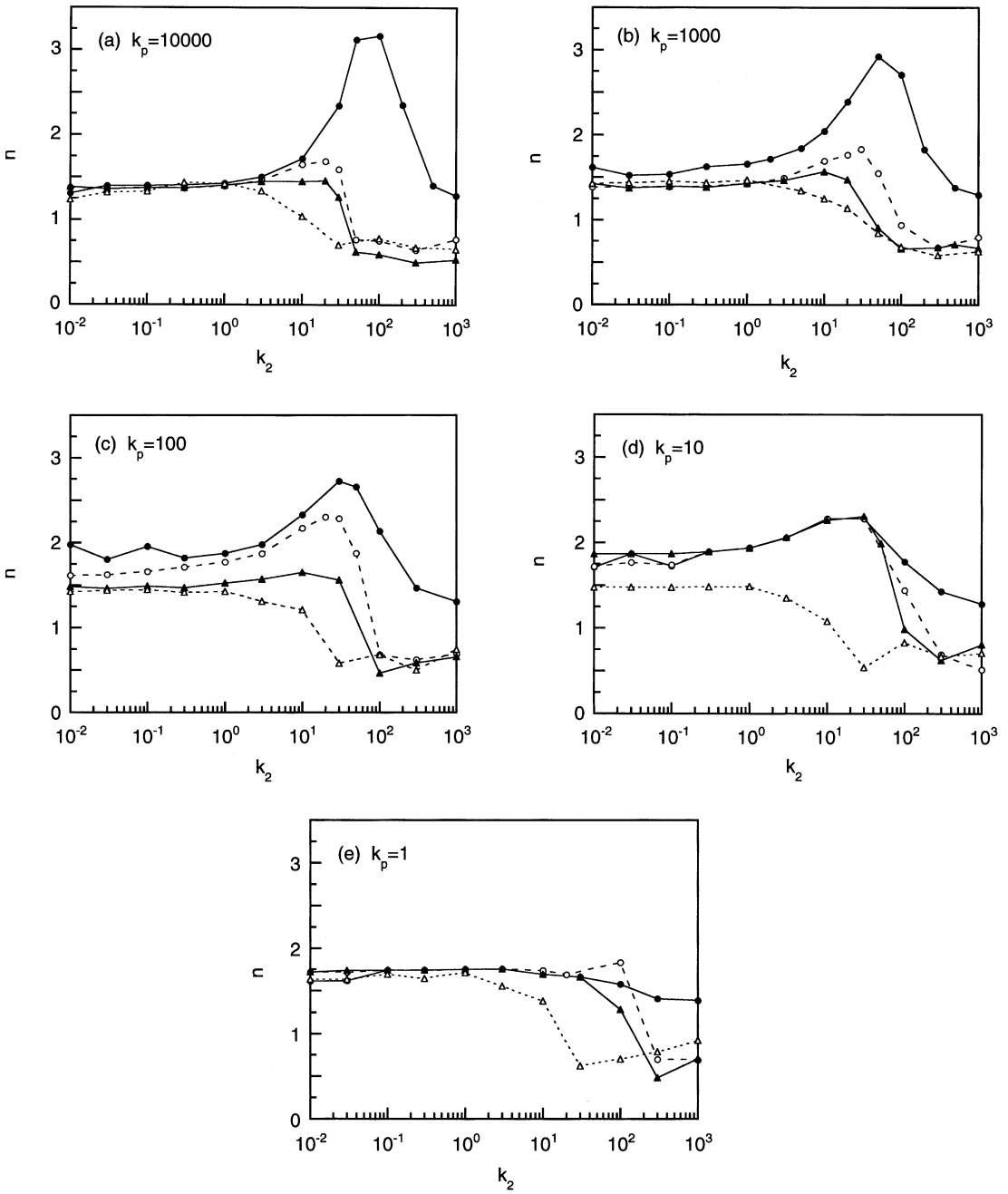

Fig. 2. Relation between k_2 and n: $k_p = 10\,000$ (a); 1000 (b); 100 (c); 10 (d) and 1 (e); $N = \infty$ (●), 200 (○), 100 (▲) and 20 (△).

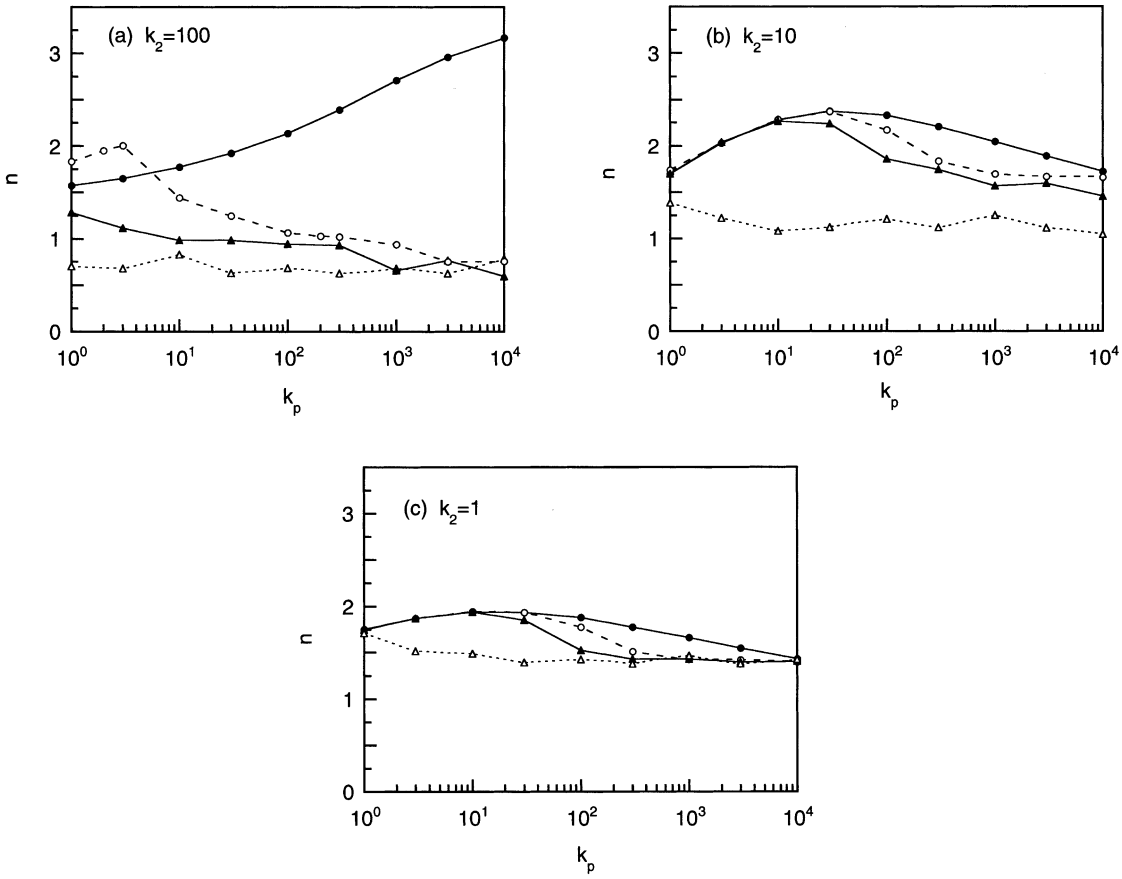

Fig. 3. Relation between k_p and n: $k_2=100$ (a); 10 (b) and 1 (c); $N=\infty$ (●), 200 (○), 100 (▲) and 20 (△).

to the constant level ($\approx 1.7\times10^{-2}$), followed by the increase in fibril formation [f(%)]. A similar tendency is observed at $k_2=1$ (Fig. 5b). At $k_2=100$ (Fig. 5c), however, the kinetic mode is different from those of smaller k_2. Firstly, [M_1] does not decrease so drastically as that at $k_2=0.01$ and 1. Actually, [M_1] remains at approximately 40 in the quasi-equilibrium (time <0.1). Secondly, the lag time before the start of the nuclear (M_{10}) formation is more clearly observed than those for $k_2=0.01$ and 1, which results in more distinct sigmoidal shapes of [P] and f at $k_2=100$, leading to the increase in the n value (Fig. 2a). When k_2 is further increased to 1000 (Fig. 5d), [M_1] has the quasi-equilibrium concentration (≈ 80) higher than the one (≈ 40) for $k_2=100$ (Fig. 5c). It should be emphasized that fundamental difference exists in the time–course of [M_{10}] between these two systems. Namely, at $k_2=1000$ the nucleus (M_{10}) is quickly formed in an early stage and then decreased slowly, which makes the sigmoidal characteristics of [P] and f less clear ($n=1.3$) than those at $k_2=100$ ($n=3.2$).

3.5. Contour map of n

It is instructive to make a contour map (Fig. 6) to show the dependency of n on k_2 and k_p. Notably, there are special regions that afford large n values at approximately $k_2=100$ and $k_p=10\,000$ for $N=\infty$ (Fig. 6a), at approximately $k_2=k_p=10$ for $N=200$ or 100 (Fig. 6b and c) and at $k_2<1$ and $k_p<$

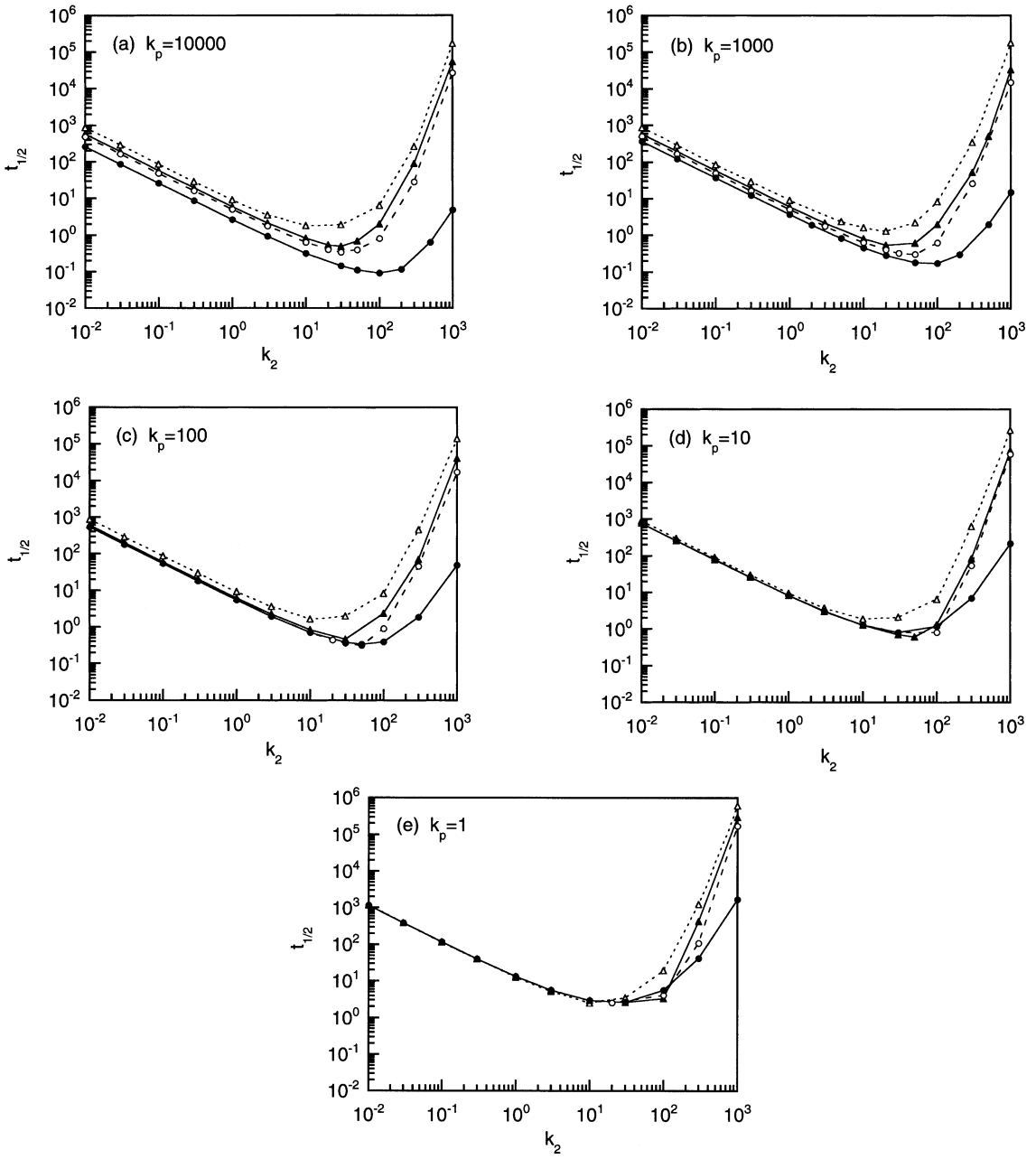

Fig. 4. Relation between k_2 and $t_{1/2}$: $k_p = 10\,000$ (a); 1000 (b); 100 (c); 10 (d) and 1 (e); $N = \infty$ (●), 200 (○), 100 (▲) and 20 (△).

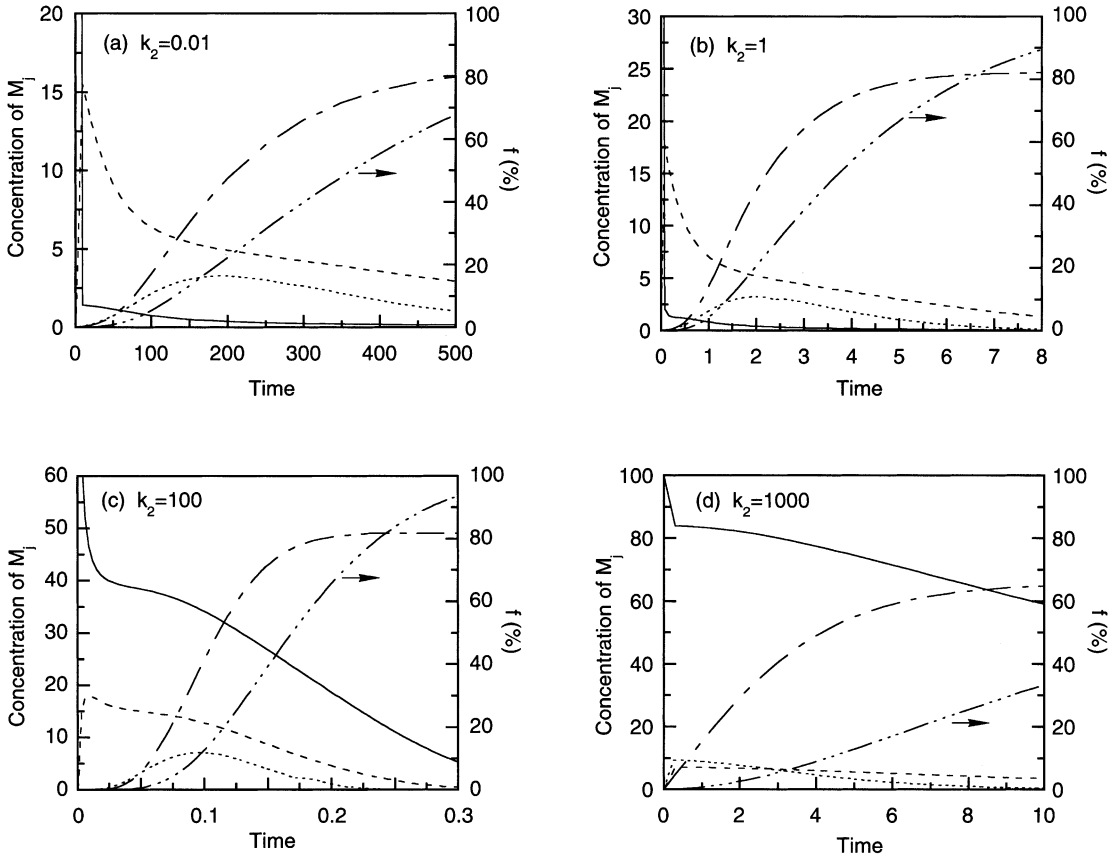

Fig. 5. Time-course concentrations of some typical species for $k_p = 1000$ and $N = \infty$: (a) 10^2 [M_1] (—), [M_2] (---), 5×10^4 [M_{10}] (···), 10^3[P] (-•-), f (-···-); (b) [M_1] (—), [M_2] (---), 5×10^4 [M_{10}] (···), 3×10^2[P] (-•-), f (-···-); (c) [M_1] (—), [M_2] (---), 10^6 [M_{10}] (···), 2×10^3[P] (-•-), f (-···-); (d) [M_1] (—), [M_2] (---), 5×10^{10} [M_{10}] (···), 10^6[P] (-•-), f (-···-).

10 for $N = 20$ (Fig. 6d). This means that as N decreases from ∞ to 20 the maximum area is moved from large k_2 and k_p values toward smaller ones.

3.6. Time-course of $k_1[M_1]/k_2$ change

The ratio of $k_1[M_1]$ and k_2 is a noteworthy parameter, since this represents the equilibrium constant between the successive species in the nucleation phase. Fig. 7 illustrates the time–course change of $k_1[M_1]/k_2$ for various k_2 values under $k_p = 1000$ and $N = \infty$, and Fig. 8 shows the relation between $k_1[M_1]/k_2$ at quasi-equilibrium state and k_2. As already shown in Fig. 2, striking sigmoidal character is observed in the cases of $k_2 = 50$ (d) and $k_2 = 100$ (e), whose $k_1[M_1]/k_2$ values are close to 0.5 in the quasi-equilibrium state. The other cases (a), (b), (c), (f) and (g) with $k_1[M_1]/k_2$ far from these values, however, do not give large sigmoid. Consequently, it seems very likely that $k_1[M_1]/k_2$ dominates the degree of sigmoidal character.

4. Discussion

A stretched exponential function (Eq. (13)) has been used in various other systems such as the Avrami's approach in crystallization [7] and the time-to-tumor model in occurrence of cancer [8]. It is generally known that a stretched exponential function describes a relaxation system in which

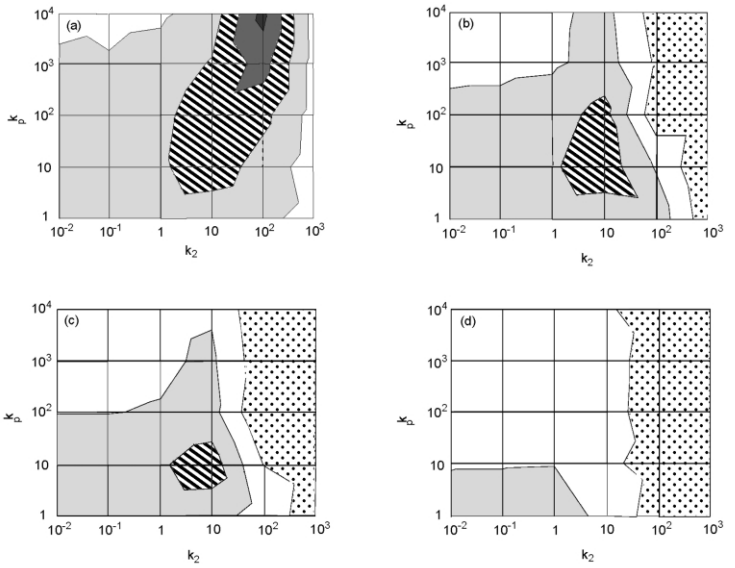

Fig. 6. Contour map describing the dependency of n on k_2 and k_p: $N = \infty$ (a); 200 (b); 100 (c) and 20 (d); n = 0.5-1 (▨), 1-1.5 (□), 1.5-2 (▩), 2-2.5 (▧), 2.5-3 (■), 3-3.5 (■).

individual components are not independent and interact with each other [9]. Actually, in the nucleation-dependent polymerization model, the aggregation proceeds in the form of cooperative sequential associations. When the individual components are independent, on the other hand, the relaxation process can be described by a simple exponential function (i.e. the case of $n=1$ in Eq. (13)). Phenomenally, the parameter n obviously reflects the cooperativity of aggregation, though it is not easy to show the physical meaning of n.

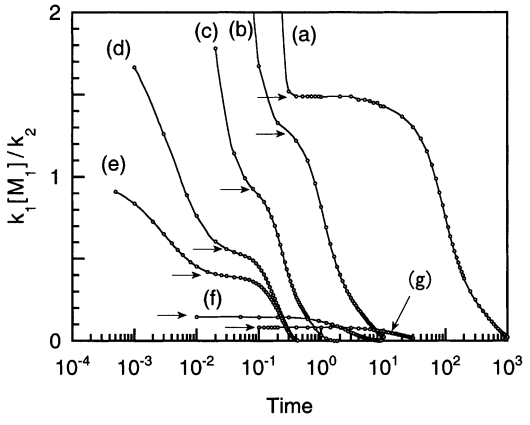

Fig. 7. Time–course change of the ratio $k_1[M_1]/k_2$ for $k_p = 1000$ and $N = \infty$: $k_2 = 0.01$ (a); 1 (b); 10 (c); 50 (d); 100 (e); 500 (f) and 1000 (g). The arrows show the positions of quasi-equilibrium states.

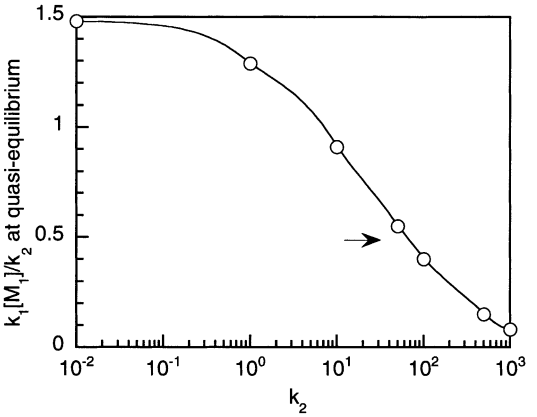

Fig. 8. Relation between $k_1[M_1]/k_2$ and k_2 for $k_p = 1000$ and $N = \infty$. The arrow indicates the region giving the large n values.

The finding that there are the optimum k_2 and k_p values generating the large n values is not compatible with the conventionally accepted interpretation in the nucleation-dependent polymerization model. The conventional idea insists that the driving force to induce sigmoidal shapes is very large k_2 and k_p values; namely, the equilibrium should lie so far to the dissociation in the nucleation step and it should lie so far to the association in the elongation step [5,6]. However, the present study has clearly revealed that the situation is not so simple as generally believed thus far. Actually, the sigmoidal character becomes small when k_2 is too large. The effect of k_2 is clearly shown in Fig. 5, where drastic change occurs between $k_2=100$ (Fig. 5c) and $k_2=1000$ (Fig. 5d). At $k_2=100$, the intermediate species emerge successively; i.e. the time (t) providing the maximal concentration is in the order of $t(M_2)<\cdots<t(M_{10})$. In contrast to this, at $k_2=1000$ the concentrations of all the intermediates (M_2–M_{10}) show the peaks almost at the same time. This marked difference in the generation of the nucleus (M_{10}) can account for the dependence of the time–course formation of [P] (the concentration of the fibril) on k_2. Since the change in [M_1] is not so large during the quasi-equilibrium, the slope of the [P] curve is almost proportional to [M_{10}] in view of Eq. (10). Therefore, the maximum slope of the [P] curve corresponds to the peak of the [M_{10}] curve. At $k_2=100$, the peak of [M_{10}] emerges after the smaller intermediate species appear, resulting in the large sigmoidal behavior of [P]. At $k_2=1000$, on the other hand, the peak of [M_{10}] appears in the early stage together with the small intermediate species, which makes the sigmoidal character of [P] small. Since [M_{10}] is very small compared with [P], $d[F]/dt$ is nearly equal to $k_p[M_1][P]$ (Eq. (11)). Therefore, the sigmoidal character of the f curve becomes large at $k_2=100$ and small at $k_2=1000$.

As mentioned in Section 3, the optimum value of $k_1[M_1]/k_2$ has turned out to be somewhat smaller than unity (~ 0.5). Since $k_1[M_1]/k_2$ means the equilibrium constant between the successive species in the nucleation phase, the above-mentioned result indicates that the nucleation phase is thermodynamically uphill to some extent. However, when k_2 value is too large and thus the nucleation phase is quite unfavorable thermodynamically, sigmoid almost disappears. Namely, prominent sigmoidal time–course appears when k_2 is larger than $k_1[M_1]$ in some degree, where [M_1] is the quasi-equilibrium concentration. This is a noticeable new result, because unfavorable nucleation due to large k_2 is generally believed to be the reason for sigmoidal curves. However, since quasi-equilibrium state [M_1] is dependent on k_2 as shown in Fig. 5, it is not easy to obtain an analytical direct relation between k_1 and k_2 necessary for inducing prominent sigmoidal time–course.

5. Conclusions

The following two conditions are necessary to obtain a remarkable sigmoidal curve in the nucleation-dependent polymerization model.

1. The elongation (extension) phase should be much longer than that of the nucleation phase; namely, $N \gg 10$ in the present system.
2. The rate constants (k_2 and k_p) should have the optimal values. Especially, k_2 should have the magnitude leading to the optimum $k_1[M_1]/k_2$ in quasi-equilibrium state, where the nucleation phase is slightly uphill from the thermodynamic point of view.

References

[1] E.A. Eckman, M. Watson, L. Marlow, K. Sambamurti, C.B. Eckman, Alzheimer's disease β-amyloid peptide is increased in mice deficient in endothelin-converting enzyme, J. Biol. Chem. 278 (2003) 2081–2084.
[2] P.M. Gorman, C.M. Yip, P.E. Fraser, A. Chakrabartty, Alternate aggregation pathways of the Alzheimer β-amyloid peptide: Aβ association kinetics at endosomal pH, J. Mol. Biol. 325 (2003) 743–757.
[3] H. Rezaei, Y. Choiset, F. Eghiaian, et al., Amyloidogenic unfolding intermediates differentiate sheep prion protein variants, J. Mol. Biol. 322 (2002) 799–814.
[4] D.L. Vanik, W.K. Surewicz, Disease-associated F198S mutation increases the propensity of the recombinant prion protein for conformational conversion to scrapie-like form, J. Biol. Chem. 277 (2002) 49065–49070.
[5] J.T. Jarrett, P.T. Lansbury Jr., Seeding 'One-dimensional crystallization' of amyloid: a pathogenic mechanism in Alzheimer's disease and scrapie?, Cell 73 (1993) 1055–1058.

[6] J. Hofrichter, P.D. Ross, W.A. Eaton, Kinetics and mechanism of deoxyhemoglobin S gelation: a new approach to understanding sickle cell disease, Proc. Nat. Acad. Sci. USA 71 (1974) 4864–4868.
[7] M. Avrami, Kinetics of phase change. II, J. Chem. Phys. 8 (1940) 212–224.
[8] A. Dewanji, D. Krewskid, M.J. Goddard, A Weibull model for the estimation of tumorigenic potency, Biometrics 49 (1993) 367–377.
[9] C. Hashimoto, H. Ushiki, Graphical analysis in gels morphology I. General method, Polym. J. 32 (2000) 807–816.